Regional activation within the vastus medialis in stimulated and voluntary contractions

Gallina, Alessio; Ivanova, Tanya D.; Garland, S. Jayne

DOI:
10.1152/japplphysiol.00050.2016

Document Version
Peer reviewed version

Citation for published version (Harvard):
Gallina, A, Ivanova, TD & Garland, SJ 2016, 'Regional activation within the vastus medialis in stimulated and voluntary contractions', *Journal of Applied Physiology*, vol. 121, no. 2, pp. 466-474. https://doi.org/10.1152/japplphysiol.00050.2016

Regional activation within the vastus medialis in stimulated and voluntary contractions

Alessio Gallina[1], Tanya D Ivanova[2], S Jayne Garland[2].

[1] Graduate program in Rehabilitation Science, University of British Columbia, Vancouver, Canada

[2] Department of Physical Therapy, University of British Columbia, Vancouver, Canada

Corresponding author: S. Jayne Garland, PhD PT

University of British Columbia, Department of Physical Therapy

212 Friedman Building, 2177 Wesbrook Mall

Vancouver, BC Canada V6T 1Z3

Email: Jayne.garland@ubc.ca

Abstract: 250 words.

New & Noteworthy: 75 words.

Text: 5596 words.

Figures: 7

Keywords: Quadriceps, Electromyography, Muscle activation, Stimulation, M-wave.

ABSTRACT:

This study examined the contribution of muscle fiber orientation at different knee angles to regional activation identified with high-density surface electromyography (HDsEMG). Monopolar HDsEMG signals were collected using a grid of 13x5 electrodes placed over the vastus medialis (VM). Intramuscular electrical stimulation was used to selectively activate two regions within VM. The distribution of EMG responses to stimulation was obtained by calculating the amplitude of the compound action potential for each channel; the position of the peak amplitude was tracked across knee angles to describe shifts of the active muscle regions under the electrodes. In a separate experiment, regional activation was investigated in ten knee flexion-extension movements against a fixed resistance. Intramuscular stimulation of different VM regions resulted in clear differences in amplitude distribution along the columns of the electrode grid ($P < 0.001$); changes in knee angle resulted in consistent shifts along the rows ($P < 0.01$) and negligible shifts along the columns of the electrode grid. Regional VM activation was identified in dynamic movement, with distal shifts of the EMG distribution in the eccentric phase of the movement ($P < 0.05$) and at more flexed knee angles ($P < 0.05$). HDsEMG was used to describe regional activation across the VM that were not attributable to anatomic factors. Changes in muscle fiber orientation associated with knee joint angle mainly influence the amplitude distribution along the fiber direction. Future studies are needed to understand possible functional roles for regional activation within the VM in dynamic tasks.

NEW & NOTEWORTHY:

This study showed, for the first time, that regional activation induced by intramuscular stimulation in vastus medialis is relatively unaffected by changes in knee angle. When examined in voluntary dynamic contractions, there were shifts in regional activation that were not attributable to anatomic factors. The

41 difference in EMG amplitude distribution between concentric and eccentric contractions provides
42 preliminary evidence that regions within the VM can be preferentially recruited according to the
43 mechanical demands of the task.

INTRODUCTION:

The activation of different regions within the vastus medialis (VM) is known to affect knee extension (proximal VM) and patellar tracking (distal VM) (14). For this reason, proximal and distal VM are often considered as separate muscles (10, 17, 22). Surface electromyography is one of the techniques commonly used to characterize quadriceps activation patterns during functional activities and exercise. However, the interpretation of the electromyographic (EMG) signals can be complicated by factors unrelated to the level of muscle activation (16). For instance, crosstalk (i.e. EMG activity originating far from the target muscle) between quadriceps heads has been previously described (2); but no detailed information about recordings from specific regions within the muscle has been reported to our knowledge. Extraction of activation patterns is also complicated in dynamic contractions, as the orientation of the muscle fibers in quadriceps changes with the knee angle (4), and this was acknowledged as a limitation in studies that analyzed regional activation within the rectus femoris during cycling (25) and walking (24). Thus more information on how changes in muscle fiber orientation influence surface EMG is needed.

High-density surface electromyography (HDsEMG) may be helpful to improve the estimation of VM regional activation in dynamic contractions. HDsEMG comprises several small electrodes arranged in a two-dimensional grid placed over the studied muscles. As the electrodes are closely spaced, it is possible to identify where the main source of EMG activity is localized (5) and to describe how the EMG amplitude decreases in space (23). In addition, when electrodes along the muscle fibers are considered, information on the position of the innervation zone can be obtained (1, 8), and it was suggested that the innervation zone can be used to track changes in muscle fiber position (4). In isometric contractions of the trapezius muscle, changes in amplitude distribution along the columns and the rows of the EMG electrode grid were previously suggested to be related to anatomical factors and regional activation,

respectively (7). A similar approach may be used to describe whether shifts in spatial amplitude distribution can be observed in different directions when they occur as a result of regional activation versus when the same region is activated but appears in a different location on the grid because of changes in the muscle fiber orientation with respect to the surface electrodes.

The purpose of this study was to examine the contribution of changes in muscle fiber orientation occurring at different knee angles to any regional activation identified with HDsEMG. To do so, two regions within the VM were selectively activated at different knee angles using intramuscular electrical stimulation. Intramuscular stimulation has the advantage of activating a consistent, selective area of the muscle. This enables the separation of the effect of regional activation (stimulation of different regions within the muscle) from changes in fiber orientation (stimulation of the same muscle region at different knee angles) on the HDsEMG recordings. Shifts in HDsEMG distribution during voluntary dynamic contractions would then need to be observed in the same direction as the regional activation induced by electrical stimulation to be considered as true regional activation.

We anticipated that: i) intramuscular stimulation of two regions within the VM would result in localized activation of muscle fibers in those regions and be observed as different EMG amplitude distributions along the columns of the EMG electrode grid; ii) changes in knee angle would result in small shifts of each EMG amplitude distribution along the rows, and no shift along the columns of the EMG electrode grid. In the dynamic contractions, we hypothesized that changes in HDsEMG amplitude distribution would be observed along the columns of the EMG electrode grid.

METHODS:

Participants

Twenty-two healthy individuals participated in this study, ten in the intramuscular stimulation protocol and twelve for the dynamic contractions protocol. Participants were included if they were older than 19 years old and if they reported no known neuromuscular disorders or recent injury. Each individual signed a written informed consent form. The study conformed to the standards set by the latest revision of the *Declaration of Helsinki* and was approved by the University of British Columbia Clinical Research Ethics Board **(H14-02035)**.

Experimental set-up

Participants sat in the Biodex dynamometer chair (System 4 Pro, Biodex Medical Systems, Shirley, NY, USA) with the lower leg (randomly selected) strapped to the knee attachment for the duration of data collection. Placement of the HDsEMG grid and the stimulation electrodes occurred with the lower limb in a standard position (sitting with hip flexed at 100 degrees and knee flexed at 90 degrees) and was guided by anatomical references. The fiber orientation of two muscle regions within the VM and its medial and lateral edges were identified using an ultrasound imaging system (LogicScan 64 LT-1T, Telemed, Vilnius, Lithuania) and were marked on the skin.

The innervation zone was located using a linear electrode array (16 silver bar electrodes, 10mm inter electrode distance, OTBioelettronica, Torino, Italy) positioned over different regions of the VM while the participants maintained a low-force isometric knee extension. The innervation zone, identifiable as phase opposition of the propagating action potentials, was oriented diagonally across the VM (i.e: aligned from medial-distal to proximal-lateral, fig. 1; see also (8, 9) and was marked on the skin. The HDsEMG grid (semi-disposable adhesive matrix; OTBioelettronica, Torino, Italy) consisted of 64 electrodes arranged in 5 columns and 13 rows (an electrode missing in one of the corners), spaced 8 mm with a total area covered by the electrodes: 96x32 mm. The position of the electrode grid was determined according to the following anatomical references: i) innervation zone aligned between the

111 2nd and 3rd column; ii) center of the grid placed approximately halfway between the medial and distal
112 edge of the VM. The grid was held in place using bi-adhesive foam, and conductive paste (Ten20,
113 Weaver and Co., Aurora, CO, USA) ensured an optimal electrical contact between the skin and the
114 electrodes. Two reference electrodes (2x3.5cm; conductive hydrogel; Kendall, Covidien, Mansfield, MA,
115 USA) were placed on the patella and on the medial side of the knee. Motor unit action potentials are
116 generated in the innervation zone and then propagate along the muscle fibers, hence the monopolar
117 EMG activity detected over the innervation zone represents the activation of the whole fiber. As VM
118 fibers are parallel to the skin, the EMG signals collected with HDsEMG in this study are representative of
119 the activation of a VM region larger than the grid itself.

120 Intramuscular stimulation of VM was performed using two insulated Teflon-coated stainless steel fine
121 wire electrodes. Each electrode consisted of a 50 μm diameter wire (California Fine Wire Company, CA,
122 USA) with 3 mm of the insulation stripped at the tip and threaded through a disposable 3.5 cm long, 25
123 gauge hypodermic needle (Becton Dickinson and Company, Franklin Lakes, NJ, USA) for intramuscular
124 insertion. A small hook was made at the terminal end of the fine wire electrode that held the electrode
125 in place after the needle was removed. All wire electrodes and hypodermic needles were sealed and
126 autoclaved in an AMSCO Sterilizer (STERIS Corporation, Mentor, Ohio, USA) for 45 min at 120º C prior to
127 use. Because electrical stimulation performed close to the neuromuscular junction requires lower
128 intensities than stimulation applied to other locations within the muscle (18), the insulated tip of the
129 wire was placed close to the innervation zone (as identified above) by puncturing the skin approximately
130 25 mm distal to the innervation zone, and advancing the needle at a constant angle of 45 degrees to the
131 skin surface following the muscle fiber orientation previously determined. As shown in fig. 1, the
132 electrodes were inserted approximately 40 mm apart, close to electrode rows 5-6 (defined: proximal
133 stimulation site) and rows 10-11 (defined: distal stimulation site). . The stimulation was applied in
134 monopolar modality with single square pulses of 10 μs duration, using the wire as the cathode and a

large carbon stimulating electrode (5x10 cm), placed on the back of the thigh as the anode. Stimulation was conducted through a constant-voltage stimulator (Grass S88, Natus Neurology Inc. - Grass Products, Warwick, RI, USA) with a stimulus isolation unit triggered by a digital interface (Power 1401 with Spike2 software, Cambridge Electronic Design, Cambridge, UK).

Anatomical reference

Anatomical references are illustrated in fig. 1. Shifts in EMG amplitude distribution will be described as "along the columns", when aligned with the long dimension of the HDsEMG grid with high row numbers being distal and low row numbers being proximal; or "along the rows", when aligned with the short dimension of the HDsEMG grid, with electrodes closer to the kneecap being lateral and away from the kneecap being medial. It should be noted that the grid used in this experiment did not cover all the innervation zones of the VM motor units. For this reason, throughout the manuscript the terms "proximal" and "distal" do not refer to the VM as a whole but rather as relative to the area of the muscle examined with the HDsEMG system.

Intramuscular stimulation protocol

Intramuscular electrical stimulation of two sites within the VM was delivered at 5, 30, 60, or 90 degrees of knee flexion (0 equals to full extension). In addition, to examine the effect of tendon slack on the EMG amplitude distribution, the stimulation was applied at rest or while the participant was maintaining a low-force background contraction. The stimulation intensity was set just above motor threshold for all knee angles (as determined by the presence of a visible muscle twitch); however, the stimulation amplitude could differ between the wires and when the stimulation was applied at rest or with a background contraction. The pulses were delivered approximately 2 s apart. Ten stimuli were delivered in each stimulation location at 4 different knee angles, repeated with/without background contraction. The testing order of the four knee angles was randomized. The knee joint angle was set using the

Biodex dynamometer in isometric mode. The amplitude of the background contraction was standardized based on the surface EMG. As knee extension torque may be produced by activating different synergists, feedback based on EMG rather than force was used to standardize VM activation. Participants were asked to maintain a contraction level of approximately 50 μV, which resulted in a knee extension torque between 5% and 10% of the maximal voluntary contraction (MVC); the MVC was measured three times with the knee at 90 degrees of flexion at the end of the protocol.

Dynamic contractions protocol

Participants sat in the Biodex chair with their hip flexed 100 degrees and performed three knee extension isometric MVCs with their knee flexed at 45 degrees. Then the Biodex was set to provide an isotonic resistance equal to 10% of the isometric MVC during knee flexion-extension movements. The participants practiced performing smooth knee flexion-extensions from 90 to 10 degrees of knee flexion for 5-8 trials. The protocol consisted of ten cycles of 3s concentric knee extension, 3s eccentric knee flexion, 3s rest. The timing was standardized using a metronome.

Data analysis

Electromyographic signals were collected in monopolar modality using a HDsEMG amplifier (128-channel EMG-USB; OTBioelettronica, Torino, Italy). Signals were amplified 200-500 times and digitized at 2048 samples/s using a 12 bit A/D converter. Before data processing, signals were band-pass filtered (10-400 Hz) using a 4^{th} order Butterworth filter. Channels with noise or artifacts due to bad skin-electrode contact (approximately 1-2 channels per participant) were identified through visual inspection and replaced with the linear interpolation of the adjacent channels. Stimulation onset (intramuscular stimulation protocol) or knee angle (dynamic contraction protocol) signals were also digitized with the same EMG acquisition system.

All data analysis was performed in Matlab R2013b (The MathWorks, Inc., Natick, MA, USA). In the intramuscular stimulation protocol, the onset of the stimulation artifact was determined by visual inspection for each participant. The stimulation artifact is easily distinguished from the compound muscle action potential as it occurs simultaneously on all the channels, whereas the first negative peak of the M-wave can be observed at different latencies in the adjacent channels along the rows because of its propagation along the muscle fiber. Samples contaminated by the stimulation artifact were excluded from the analysis. The M-waves were similar both for repeated stimulation at a single knee angle (fig.2) and at different knee angles (fig.3). For each stimulus, the amplitude of the response in each channel was defined as the peak-to-peak value of the M-wave, resulting in 64 amplitude values, which were averaged across the 10 stimuli. Afterwards, the spatial resolution of the amplitude distribution was improved by interpolation (spline, factor 8) (9, 13). With this method, a virtual grid with channels spaced 1 mm in both directions was obtained. All the amplitude distributions had a single EMG amplitude peak and values monotonically decreasing along both columns and rows of the grid; the location of this peak on the grid was determined by extracting both coordinates. The analysis of the two coordinates separately enables to characterize changes in amplitude distribution occurring along the rows from those occurring along the columns of the electrode grid. In the dynamic contractions protocol, each of the eccentric and concentric phases was split into 4 intervals of 20 degrees to provide a total of 8 intervals per trial. For each interval, an amplitude distribution was obtained by calculating the average rectified value (ARV) for each channel of the grid. As regional activation is expected to be represented by changes along the columns of the electrode grid, only the maximum of each row of 5 electrodes was considered; this created a virtual array of 13 values, describing the amplitude distribution along the columns of the grid; regional activation was described as the barycentre of the 3 channels with the highest amplitude. The activation level was quantified as the average amplitude values of the 3 channels, expressed as a percentage of the EMG activity measured during the MVC

(amplitude of the 4 highest amplitude values). Also, to characterize the amount of EMG activity measured by the top three electrodes in comparison to the 13-channel distribution, the difference between amplitude of the peak and that of the other channels was quantified as: $100*(M_3 - M_{13})/M_3$, where M_3 is the average amplitude of the three highest channels and M_{13} is the average of the 13 values.

In a secondary analysis, we determined whether isometric contractions performed at different knee angles resulted in different EMG amplitude distributions. The data collected when intramuscular stimulation was applied while keeping a background activation was analyzed. M-waves (intervals from 50 ms before to 150 ms after each stimulus) were excluded from the analysis. The average rectified value (ARV) was calculated for each channel of the grid in a 15s epoch moving in steps of 250 ms. The epoch in which the average of the five largest amplitude values was closest to 50 μV was used for the analysis. The EMG amplitude distribution along the columns of the grid was quantified in the same way as for the dynamic contractions.

Statistical Analysis

For the intramuscular stimulation protocol, the decrease in amplitude with distance from the peak is reported as the mean and standard deviation at different distances from the peak. Two separate 3-way ANOVA tests were used to test the effect of *knee angle*, *stimulation location* and *background contraction* on the position of the peak of the EMG amplitude distribution along the columns and the rows of the EMG electrode grid. Amplitude data were reported as the peak-to-peak value (positive and negative deflections). To ensure that the stimulation artifact that periodically covered part of the onset of the M-wave did not influence the results of these analyses, 3-way ANOVA tests were applied also on the coordinates extracted from the second, positive peak only. As the main results of the two analyses are comparable, only data for peak-to-peak amplitudes are reported.

For the dynamic contractions protocol, the effect of *knee angle* and *contraction type (*concentric*,* eccentric*)* on the position of EMG amplitude distribution along the columns of the grid was tested using 2-way ANOVA. Because the amplitude distribution may be influenced by the activation level, the same test was also run on the normalized EMG amplitude to test whether knee angle and contraction type influence the amount of muscle activation.

For both experiments, statistical analyses were performed using SPSS v. 22 (IBM Inc., Armonk, NY, USA). All factors were considered as within-subject. The assumption of normally-distributed data (Shapiro-Wilk test) was met for all tests; when sphericity (Mauchly's test) was not assumed, a Greenhouse-Geisser correction was applied. Bonferroni corrections were applied to post-hoc pairwise comparisons. Post-hoc analysis of the factor *angle* in the dynamic contractions protocol was performed across the 4 levels using a contrast analysis (12).

For the isometric contractions, the effect of *knee angle* on the position of EMG amplitude distribution along the columns of the grid was tested using the Friedman test because the data were not normally distributed. Post-hoc pairwise comparisons were run using paired Wilcoxon tests with Bonferroni correction.

Comparisons that identified shifts in the amplitude distribution smaller than half an interelectrode distance (< 3.5 mm) are not reported as such small shifts are below the spatial resolution of the electrode grids. The statistical significance was set at $P < 0.05$.

RESULTS:

Participants

Ten participants took part in the intramuscular stimulation protocol (3 female; 30 ± 11 years old; height: 180.7 ± 8.2 cm; weight: 75.9 ± 12.6 kg) and twelve in the dynamic contractions protocol (10 female; 27 ± 4 years old; height: 172.2 ± 9.5 cm; weight: 63.0 ± 12.4 kg).

Intramuscular stimulation protocol

Each M-wave was biphasic with an initial negative deflection, partially covered by the stimulation artifact, and a second positive peak. Different latencies across channels due to propagation of the action potential could be observed for the negative but not for the positive peak (fig. 2 and 3), and this helped identify M-waves from artifacts (highlighted in fig. 3). In the channel with the largest response, the latency was on average 14.7±0.9 ms and 28.3±3.1 ms for the negative and positive peaks, respectively. The M-wave peak-to-peak value was a median of 3581 μV (25^{th} - 75^{th} percentiles: 1586 – 7868 μV). The variability of the responses across the ten stimuli was negligible (fig. 2). Figure 3 illustrates M-waves at all the angles tested.

Changes in M-wave amplitude with distance

Each stimulation resulted in a single, well-defined peak of activity in the EMG amplitude distribution (fig. 4A). From this peak activity, the amplitude decreased monotonically both along rows and columns of the grid. The average decrease in EMG amplitude with distance from the peak averaged across participants is shown in fig. 4B. When normalized to the peak amplitude, monopolar EMG signals recorded one interelectrode distance (8 mm) away from the peak were on average 90.1±6.2% of the maximum amplitude. Amplitude further decreased with distance to 71.2±11.0% at 16 mm, 51.9±12.5% at 24 mm and became less than 10% (9.9±4.9%) of the peak value at a distance of 64 mm from the peak.

Intramuscular stimulation

The position of the maximum EMG peak-to-peak amplitude was analyzed for the "along the columns" and the "along the rows" coordinates separately (fig. 5). For the direction "along the columns" (fig. 5A), stimulation applied to the proximal site resulted in EMG activity localized on average 47.3 mm more proximal than that resulting from stimulation of the distal site (F (1, 9) = 364.1, $P < 0.001$). There was an interaction effect of *knee angle* and *background contraction* (F (3, 27) = 5.6, $P < 0.01$). Post-hoc testing revealed that stimulations applied while holding a background contraction resulted in a more proximal coordinate of the EMG peak than at rest at all the knee angles ($P < 0.01$; mean difference: 3.9 mm), but no differences amongst knee angles were identified ($P > 0.06$, shift smaller than half an interelectrode distance).

For the "along the rows" direction (fig. 5B), the position of the maximum EMG peak-to-peak amplitude was influenced by *knee angle* and *background contraction* (interactive effect, F (3, 27) = 6.4, $P < 0.01$). The EMG peak shifted medially at each knee angle (post-hoc test, $P < 0.05$) except when the knee was moved from 30 to 5 degrees while holding a background contraction ($P = 0.59$). The total shift (from 90 to 5 degrees) was 6.2 mm at rest and 7.5 mm while holding a background contraction. Furthermore, the position of the EMG peak was influenced by *stimulation location* and *background contraction* (interactive effect, F (1, 9) = 6.1, $P < 0.05$). Post-hoc analysis revealed that the EMG peak amplitude was more medial for the proximal than for the distal stimulation site, more so when stimulation was applied at rest ($P < 0.05$; difference: 4.9 mm) than while holding a contraction ($P = 0.08$; difference: 3.8 mm).

Dynamic contractions

Data from representative participants are shown in fig. 6, and data pooled across participants are shown in fig. 7. On average, the region of maximal EMG amplitude was localized more distally in eccentric compared to concentric contractions ($P < 0.05$) and moved proximally ($P < 0.05$) with knee extension (linear trend, $P < 0.05$). However, this was not uniformly found in all participants (fig. 6 right panel), as

indicated by the large standard errors in fig. 7A. A proximal shift of the region of maximal EMG amplitude with more extended knee positions was observed in 9 participants out of 12 both in the concentric and in the eccentric phases; a distal shift of maximal EMG amplitude in the eccentric compared to the concentric phase of the movement was observed in 10 participants out of 12 (at 70-50 degrees). A trend for an interactive effect between *knee angle* and *contraction type* was identified (P = 0.07), and post-hoc comparisons showed that the region of maximal amplitude within the VM was more distal in the eccentric than in the concentric contraction between 30 and 70 degrees ($P < 0.05$), but not when the knee was more extended or more flexed ($P > 0.13$). The amplitude of the three highest channels was on average 14.2±6.8% higher than the average of the array of 13 amplitude values. Amplitude increased linearly with the knee angle (linear trend, $P < 0.001$). An interaction effect between *knee angle* and *contraction type* was identified for the peak amplitude (fig. 7B; $P < 0.01$) with the amplitude being higher in the concentric than in the eccentric phase of the knee extension between 30 and 10 degrees only ($P = 0.05$).

Isometric contractions:

The region of maximal amplitude within the muscle differed across joint angles ($P < 0.05$). The amplitude distribution was localized more proximally at 30 than at 90 degrees ($P < 0.017$) and there was a trend for a difference between 60 and 90 degrees ($P = 0.022$) and 5 and 90 degrees ($P = 0.047$); no differences were identified across the other angles.

DISCUSSION

This study demonstrated that shifts in EMG amplitude distribution associated with regional activation versus changes in muscle fiber orientation were differentially observed on the two dimensions of the electrode grid. These findings were used to interpret data on regional activation within the VM in dynamic voluntary contractions.

In this study, the activation of regions within the VM could be described in space by a single amplitude peak. Across the muscle fiber direction, both monopolar and differential surface EMG signals peak above the location of the active motor units (20); along the muscle fiber direction, monopolar EMG signals peak above the innervation zone while differentials peak twice, between the innervation zone and each tendon (19). In the current study, the columns of the EMG electrode grid were aligned to the VM innervation zone, and therefore each electrode was placed on a different group of fibers. For this reason, shifts in EMG amplitude observed along the direction of the columns indicate regional activation. Instead, the rows of the grid were placed along the approximate VM fiber direction, hence changes in EMG amplitude distribution along the direction of the rows would be related to changes in fiber orientation.

Intramuscular stimulation has two main advantages over surface stimulation. First, intramuscular stimulation can be applied at lower intensities, likely reducing the stimulation artifact. Second, because the wire was placed in the muscle, it increases the likelihood that the same groups of muscle fibers were targeted at different knee angles (fig.3). Surface stimulation electrodes would be more affected by movement of the muscle fibers with respect to the skin which could result in stimulation of different muscle fiber groups with changing knee angle. Of note, the placement of the intramuscular wire in this study ensured that most of the electrical stimulation was applied in close proximity to the fiber innervation zone, likely resulting in a direct stimulation of the neuromuscular junction or of the terminal nerve branches at low stimulus intensities. The combination of intramuscular stimulation technique and HDsEMG may also be used to study the effects of changes in muscle architecture and regional activation on the EMG signals from other muscles, as long as the innervation zone can be properly located. Another application may be for the study of localized myoelectric manifestations of fatigue in response to repetitive electrical stimulation of muscle regions.

Electrical stimulation selectively applied through intramuscular fine wire electrodes resulted in a localized peak of EMG activity. Approximately 25 mm away from the peak, the EMG amplitude was decreased by half. At more than 60 mm from the peak, the M-wave amplitude was only 10% of the largest response detected by the grid. Given that VM motor unit action potentials were shown to have localized representation on the skin, suggesting that muscle fibers innervated by individual VM motoneurons are confined to limited muscle regions (9), the amplitude distribution of the M-waves observed in this study suggests that the intramuscular electrical stimulation focally recruited motor units with muscle fibers confined to the VM region of interest.

Stimulation applied through the proximal or distal intramuscular electrode had a large effect on the amplitude distribution along the columns. The peak of EMG activity observed on the grid was close to the electrode column where the wire was inserted. This confirms that changes in regional activation within the muscle are reflected in shifts in the EMG amplitude along the columns of EMG electrode grid. The location of the intramuscular stimulation also had a small effect on the position of the EMG amplitude peak along the rows of the electrode grid, resulting in a more medial position of the EMG peak amplitude when the stimulation was applied proximally, especially at rest. Minor differences in the alignment of the electrode grid with respect to the proximal and distal innervation zones might explain this difference.

In the stimulation protocol, changes in knee angle mainly influenced the EMG amplitude distribution along the rows of the electrode grid. The total excursion of the EMG amplitude peak with the tested knee angles was close to one interelectrode distance, and it was not uniform across the knee angles. Extending the knee from 90 to 60 degrees of flexion resulted in the largest shift, followed by 60 to 30 and lastly at the final degrees of knee extension some comparisons failed to reach statistical significance. Two studies investigated changes in the position of the innervation zone along the fiber

direction at similar knee joint angles; a shift of up to 10 mm in two individuals out of three (3) and inconsistent shifts across VM regions (8) were reported. Our findings were in the same order of magnitude, suggesting that the shift in EMG amplitude distribution resulted from a proximal movement of the innervation zone with increasing knee extension. Changes in knee angle had a minor influence on the EMG amplitude distribution along the columns of the electrode grid, with a non-significant proximal shift of less than half an interelectrode distance. Notably, this shift was much smaller than that related to regional activation (six interelectrode distances), hence shifts of the EMG amplitude along the columns of the electrode grid related to changes in knee angle are unlikely to be a confounding factor in the estimation of regional activation within VM.

Holding a background contraction mainly influenced the EMG amplitude distribution along the columns of the electrode grid. The largest M-waves were localized one half of an interelectrode distance more proximally when elicited during a background contraction than at rest. A small shift was identified along the rows of the electrode grid. The inclusion of the background contraction in the testing conditions was necessary to analyze the effect of muscle and tendon slack on the position of the EMG amplitude distribution. Similar to the changes observed with altering knee angle, the relatively small shift (one half of an interelectrode distance) of the EMG amplitude distribution along the columns of the electrode grid related to holding a background contraction is unlikely to impact the estimation of changes in regional activation within the VM.

Changes in barycenter of the EMG amplitude distribution along the columns of the electrode grid were observed during dynamic knee flexion-extension contractions and in the isometric contractions at different knee angles. We suggest that in the dynamic task changes in muscle fiber orientation are unlikely to explain this redistribution. Given the results of the intramuscular stimulation protocol, these changes in amplitude distribution may be explained by preferential regional activation

within the VM. This interpretation is further strengthened by the comparison of concentric and eccentric contractions, as significant differences in the amplitude distribution along the electrode grid were observed for the same knee angles (fig. 7). While inter-subject variability in muscle anatomy (11) and in motor strategies to accomplish the task may have resulted in inconsistent patterns across individuals, pooled data showed that the amplitude distribution along the columns of the grid was localized more distally in eccentric contractions and at more flexed knee joint angles. A similar pattern was observed in the isometric contractions; differences between these findings and the non-significant ones reported in a previous study (6) are likely due to difference in protocols and data analysis. In this study, because the activation level was not different for 7 out of 8 angles tested, the difference in amplitude distribution observed between concentric and eccentric contractions cannot be attributed to differences in the intensity of muscle activation. We cannot exclude the possibility that the intensity of muscle activation had an impact on the proximal shift of the EMG amplitude with increasing knee angle in both concentric and eccentric contractions. ~~Future studies should investigate the influence of knee angle and voluntary muscle activation level separately.~~ The difference in EMG amplitude distribution between concentric and eccentric contractions provides preliminary evidence that regions within the VM can be preferentially recruited according to the mechanical demand of the task. This may reflect strategies to compensate for mechanical efficiency (e.g. regional differences in fiber shortening at different knee angles; 15, 26) and/or to take advantage of the different force vectors produced by fibers residing in different regions of the muscle (14). Future studies are needed to investigate the mechanisms and functional consequences of regional muscle activation, as well as the consistency of these strategies across healthy individuals and in clinical populations.

This study has some limitations. Some of the measures described in the intramuscular stimulation protocol were on average close to or less than half of an interelectrode distance. While these measures were calculated on signals interpolated from electrodes spaced 8 mm apart, the shift of the peak EMG

amplitude was consistent across participants and conditions. Even if the effects that identified shifts smaller than one interelectrode distance were simplified as “no shift”, the main findings of this study would not change. There was an imbalance in the number of male and female participants in the two experiments. While differences in subcutaneous adipose tissue might affect some parameters of the EMG signal, a recent study (19) showed that motor unit depth influences how widely its surface amplitude distributes on the skin but not the position of its peak amplitude, which is the main parameter of interest in this study. Furthermore, the analysis of isometric and dynamic voluntary contractions revealed similar results although being performed on two different groups of participants.

CONCLUSIONS

High-density surface electromyography revealed consistent changes in the EMG amplitude distribution associated with regional activation and changes in muscle fiber orientation. An appropriate placement of the electrode grid enabled us to distinguish regional activation (shifts of EMG amplitude distribution along the columns of the grid) from changes in muscle fiber orientation associated with changes in knee angle (shifts of EMG amplitude distribution along the rows of the grid). Shift of the EMG amplitude distribution along the columns of the electrode grid related to changes in knee angle and muscle contraction were on average negligible (less than one half of an interelectrode distance) and much smaller than the shift observed for regional activation (six interelectrode distances in this study). When used to investigate within-muscle changes in a voluntary dynamic task, this technique showed a proximal shift of the amplitude distribution in more extended knee positions and in concentric compared to eccentric contractions that likely reflects preferential activation of muscle regions in the VM.

FUNDING

Alessio Gallina was supported by a Vanier Graduate Canada Scholarship. This study was supported in part by the Natural Sciences and Engineering Research Council of Canada (S.J.G.).

AUTHORS CONTRIBUTION

Author contributions: A.G., T.D.I and S.J.G. conception and design of research; A.G., T.D.I and S.J.G performed experiments; A.G. analyzed data; A.G., T.D.I and S.J.G. interpreted results of experiments; A.G. prepared figures; A.G. drafted manuscript; A.G., T.D.I and S.J.G. edited and revised manuscript; A.G., T.D.I and S.J.G. approved final version of manuscript.

REFERENCES

1. **Beck TW**, **Housh TJ**, **Cramer JT**, **Weir JP**. The effect of the estimated innervation zone on EMG amplitude and center frequency. *Med Sci Sports Exerc* 39: 1282–1290, 2007.

2. **Farina D**, **Merletti R**, **Indino B**, **Nazzaro M**, **Pozzo M**. Surface EMG crosstalk between knee extensor muscles: experimental and model results. *Muscle Nerve* 26: 681–95, 2002.

3. **Farina D**, **Merletti R**, **Nazzaro M**, **Caruso I**. Effect of joint angle on EMG variables in leg and thigh muscles. *IEEE Eng Med Biol Mag* 20: 62–71, 2001.

4. **Farina D**. Interpretation of the surface electromyogram in dynamic contractions. *Exerc Sport Sci Rev* 34: 121–7, 2006.

5. **Gallina A**, **Botter A**. Spatial localization of electromyographic amplitude distributions associated to the activation of dorsal forearm muscles. *Front Physiol* 4: 1–8, 2013.

6. **Gallina A**, **Gazzoni M**. Selective activation of muscle sub-portions within the vastus medialis: effect of gender, knee angle and force level. *Ital J Physiother* 20–29, 2013.

7. **Gallina A**, **Merletti R**, **Gazzoni M**. Uneven spatial distribution of surface EMG: what does it mean? *Eur J Appl Physiol* 113: 887–94, 2013.

8. **Gallina A**, **Merletti R**, **Gazzoni M**. Innervation zone of the vastus medialis muscle: position and effect on surface EMG variables. *Physiol Meas* 34: 1411–22, 2013.

9. **Gallina A**, **Vieira T**. Territory and fiber orientation of vastus medialis motor units: a surface electromyography investigation. *Muscle Nerve* 52: 1057–1065, 2015.

10. **Hedayatpour N**, **Falla D**, **Arendt-Nielsen L**, **Vila-Chã C**, **Farina D**. Motor unit conduction velocity

during sustained contraction after eccentric exercise. *Med Sci Sports Exerc* 41: 1927–1933, 2009.

11. **Holt G**, **Nunn T**, **Allen RA**, **Forrester AW**, **Gregori A**. Variation of the Vastus Medialis Obliquus Insertion and its Relevance to Minimally Invasive Total Knee Arthroplasty. *J Arthroplasty* 23: 600–604, 2008.

12. **Laija W**. Conducting ANOVA Trend Analyses Using Polynomial Contrasts. *Annu. Meet. Southwest Educ. Res. Assoc. Austin,* 1997.

13. **Lapatki BG**, **Oostenveld R**, **Van Dijk JP**, **Jonas IE**, **Zwarts MJ**, **Stegeman DF**. Topographical characteristics of motor units of the lower facial musculature revealed by means of high-density surface EMG. *J Neurophysiol* 95: 342–54, 2006.

14. **Lin F**, **Wang G**, **Koh JL**, **Hendrix RW**, **Zhang L**. In vivo and Noninvasive Three-Dimensional Patellar Tracking Induced by Individual Heads of Quadriceps. *Med Sci Sport Exerc* 36: 93–101, 2004.

15. **Loeb GE**. Motoneurone task groups: coping with kinematic heterogeneity. *J Exp Biol* 115: 137–146, 1985.

16. **Merletti R**, **Rainoldi A**, **Farina D**. Surface electromyography for noninvasive characterization of muscle. *Exerc Sport Sci Rev* 29: 20–25, 2001.

17. **Pattyn E**, **Verdonk P**, **Steyaert A**, **Van Tiggelen D**, **Witvrouw E**. Muscle functional MRI to evaluate quadriceps dysfunction in patellofemoral pain. *Med Sci Sports Exerc* 45: 1023–1029, 2013.

18. **Popovic D**, **Gordon T**, **Rafuse VF**, **Prochazka a**. Properties of implanted electrodes for functional electrical stimulation. *Ann Biomed Eng* 19: 303–16, 1991.

19. **Rodriguez-Falces J**, **Negro F**, **Gonzalez-Izal M**, **Farina D**. Spatial distribution of surface action potentials generated by individual motor units in the human biceps brachii muscle. *J*

Electromyogr Kinesiol 23: 766–77, 2013.

20. **Roeleveld K**, **Stegeman DF**, **Vingerhoets HM**, **Van Oosterom A**. The motor unit potential distribution over the skin surface and its use in estimating the motor unit location. *Acta Physiol Scand* 161: 465–72, 1997.

21. **Smith TO**, **Nichols R**, **Harle D**. Do the Vastus Medialis Obliquus and Vastus Medialis Longus Really Exist? A Systematic Review. *Clin Anat* 199: 183–199, 2009.

22. **Tenan MS**, **Peng Y-L**, **Hackney AC**, **Griffin L**. Menstrual cycle mediates vastus medialis and vastus medialis oblique muscle activity. *Med Sci Sports Exerc* 45: 2151–7, 2013.

23. **Vieira TMM**, **Loram ID**, **Muceli S**, **Merletti R**, **Farina D**. Postural activation of the human medial gastrocnemius muscle: are the muscle units spatially localised? *J Physiol* 589: 431–43, 2011.

24. **Watanabe K**, **Kouzaki M**, **Moritani T**. Regional neuromuscular regulation within human rectus femoris muscle during gait. *J Biomech.* 47: 3502-8, 2014.

25. **Watanabe K**, **Kouzaki M**, **Moritani T**. Heterogeneous neuromuscular activation within human rectus femoris muscle during pedaling. *Muscle and Nerve* 52: 404–11, 2015.

26. **Windhorst U**, **Hamm TM**, **Stuart DG**. On the function of muscle and reflex partitioning. *Behav Brain Sci* 12: 629, 1989.

FIGURES:

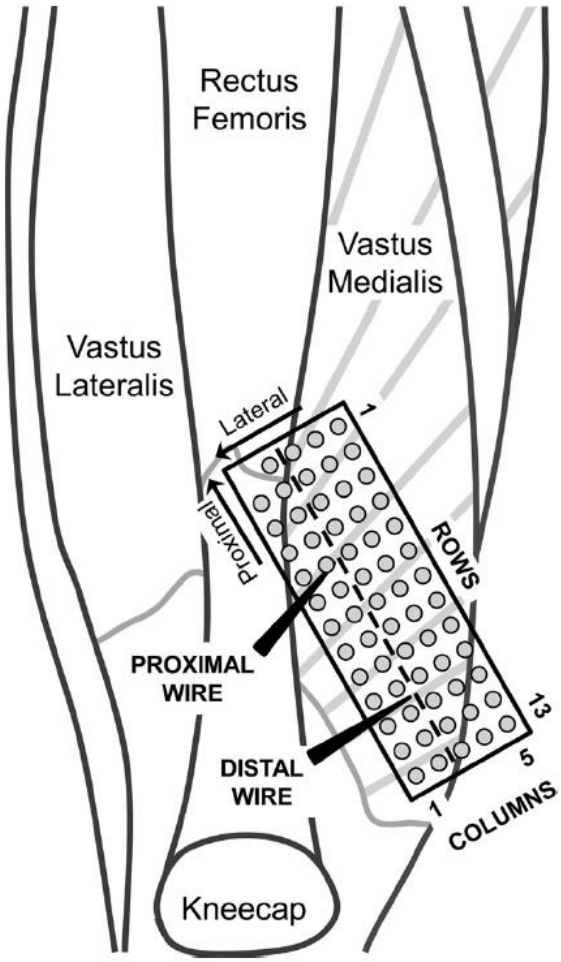

Figure 1: Experimental setup. The 64 electrode grid was placed so that the VM innervation zone (dashed line) was located between the 2nd and 3rd column of electrodes. The wires used for stimulation (black triangles) were inserted close to electrode rows number 5-6 (proximal) and 10-11 (distal). Orientation of the VM fiber was illustrated based on the data from Smith et al. (21).

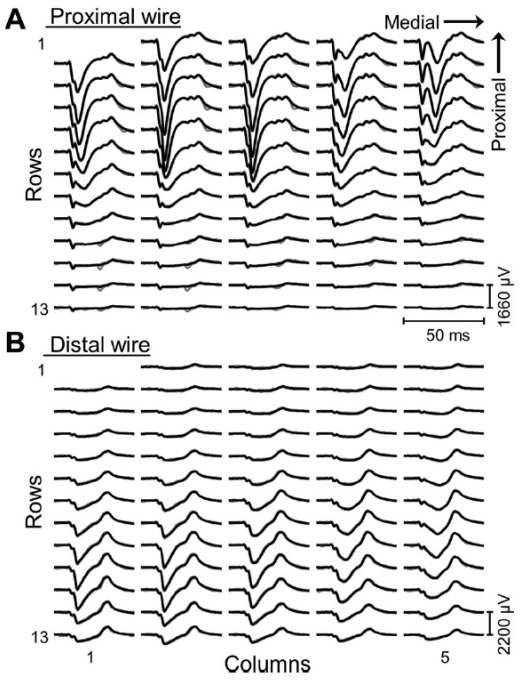

Figure 2: Example of M-waves elicited by stimulation of the proximal (A) and distal (B) muscle regions in a representative participant (knee angle: 90 degrees). Channels are organized as in the electrode grid in fig. 1. Each channel shows 10 responses superimposed. When the stimulation is applied proximally, almost no EMG activity can be observed in the distal muscle region and vice-versa.

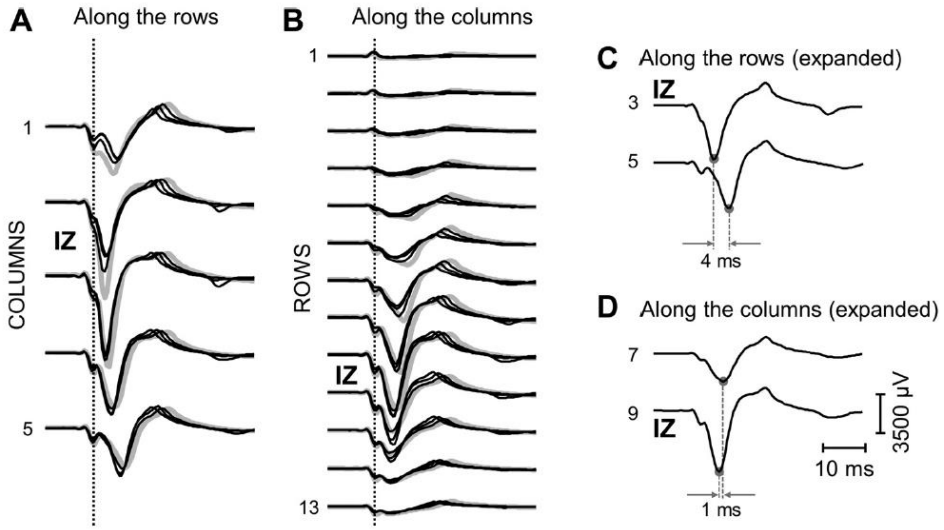

Figure 3: Example of action potentials along columns (A) and rows (B) of the grid. The stimulation artifact is highlighted (dotted lines). M-waves elicited at the four knee angles tested are superimposed; the thicker, grey lines identify stimulations at 90 degrees. In A, action potential propagation can be observed as longer latencies of the negative peak in channels far (1, 4 and 5) than channels close to the innervation zone (IZ - 2 and 3); the negative peak in column 5 occurs 4 ms later than in column 3 (detailed in panel C). This confirms that the rows of the grid were placed along the approximate VM fiber orientation. In B, the difference in latencies across channels is minimal; the negative peak in row 7 occurs 1 ms later than in row 9 (detailed in panel D). Differences in latency between positive and negative peak of each M-wave at different knee angles are likely related to changes in muscle fiber length.

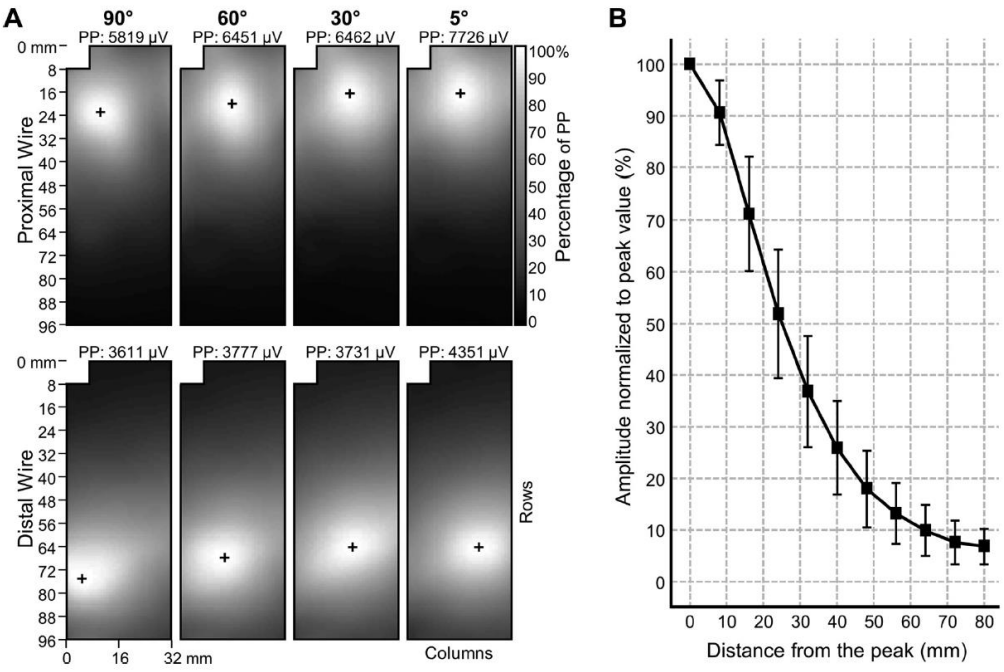

521

522 Figure 4: A) EMG amplitude distributions at different knee angles in a representative participant. The
523 gray scale of each map is normalized between 0 and its maximal value (reported on top of each panel).
524 The peak is localized more proximally (along the columns) when the stimulation is applied proximally
525 (top vs. bottom panels). A lateral-medial shift (along the rows) shift can be observed as the knee is
526 moved to a more extended position (panels on the right). B) Decrease of EMG amplitude with distance.
527 For all participants and conditions (N = 160), amplitude values were normalized to the peak, pooled
528 together and plotted as a function of the distance from the peak in steps of 8 mm (inter-electrode
529 distance). Bars indicate standard deviation.

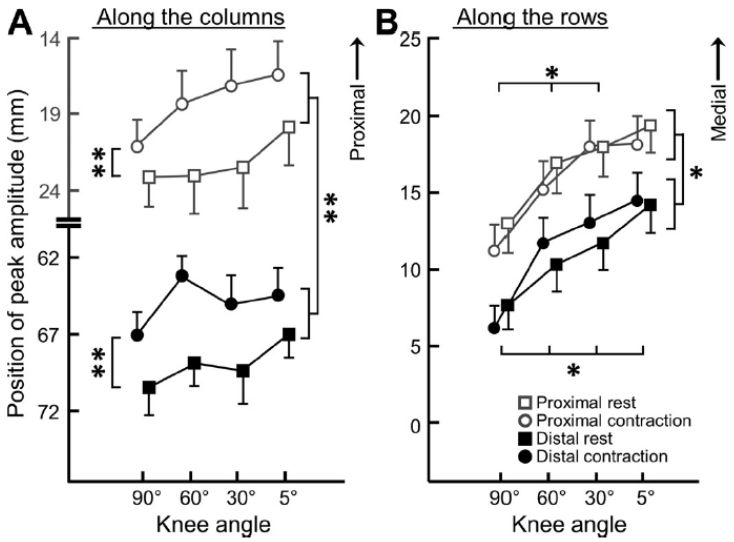

530

531 Figure 5: Shift of EMG amplitude distribution along columns (A) and rows (B) of the electrode grid.
532 Effects of stimulation site (proximal, grey; distal, black) and background contraction (rest, square;
533 background contraction, circle) can be clearly observed along the columns (A). Effects of knee joint
534 angle can mainly be observed along the rows (B). Data are mean ± standard error; * $P < 0.05$; ** $P <$
535 0.01.

536

537

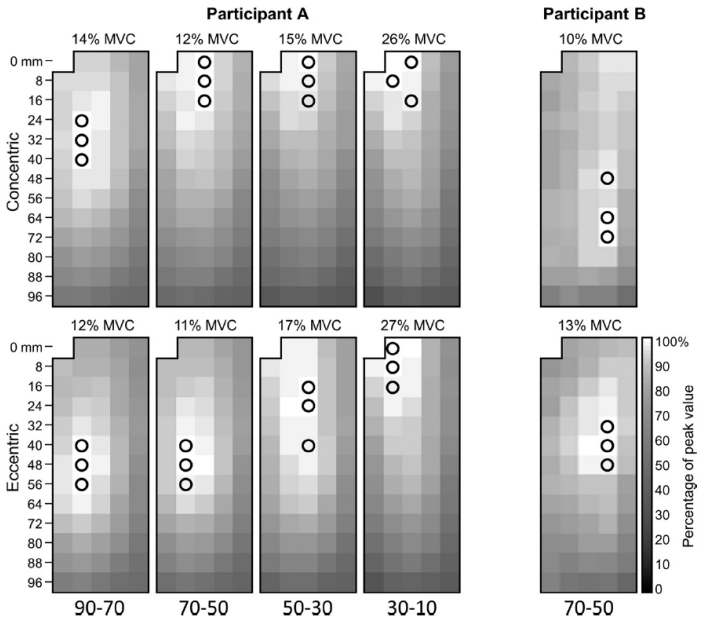

538

539 Figure 6: Examples of EMG amplitude distributions at different knee angles in the concentric/eccentric
540 phase of the dynamic contraction. The gray scale of each map is normalized between 0 and its maximal
541 value (reported on top of each panel). Black circles identify the peak channels. The peak EMG activity
542 was more proximal in the concentric phase than the eccentric phase at each knee angle for participant
543 A. Participant B shows an opposite pattern (a single knee angle is shown for illustrative purposes).

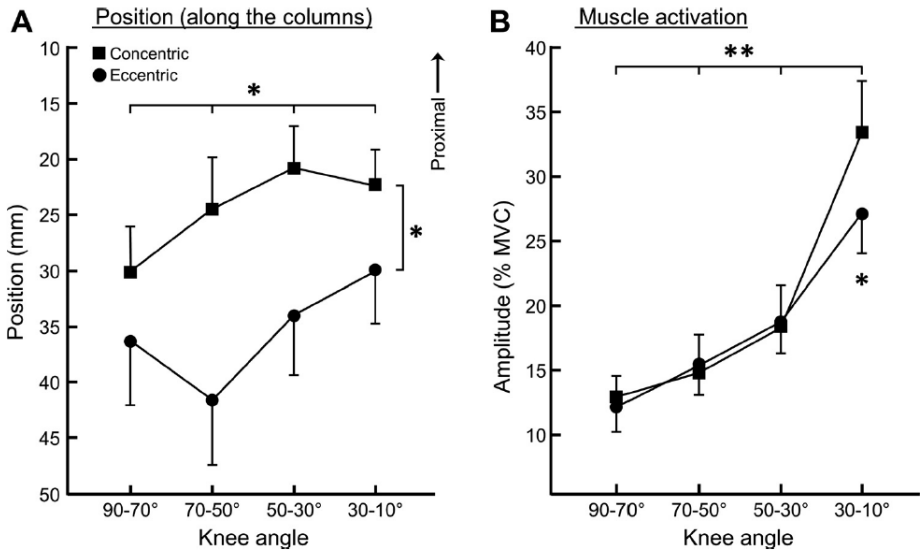

544

545 Figure 7: Peak EMG amplitude distribution along the columns of the electrode grid (A) and changes in
546 muscle activation (B) during the dynamic contractions. Phase of the movement (squares, concentric;
547 circles, eccentric) and knee angles are shown. Data are mean ± standard error; * $P < 0.05$; ** $P < 0.01$.